

Sequential and Incremental Precoder Design for Joint Transmission Network MIMO Systems with Imperfect Backhaul

Ming Ding, *Member, IEEE*, Jun Zou, Zeng Yang, Hanwen Luo, and Wen Chen, *Senior Member, IEEE*

Abstract—In this paper, we propose a sequential and incremental precoder design for downlink joint transmission (JT) network MIMO systems with imperfect backhaul links. The objective of our design is to minimize the maximum of the sub-stream mean square errors (MSE), which dominates the average bit error rate (BER) performance of the system. In the proposed scheme, we first optimize the precoder at the serving base station (BS), and then sequentially optimize the precoders of non-serving BSs in the JT set according to the descending order of their probabilities of participating in JT. The BS-wise sequential optimization process can improve the system performance when some BSs have to temporarily quit the JT operations because of poor instant backhaul conditions. Besides, the precoder of an additional BS is derived in an incremental way, i.e., the sequentially optimized precoders of previous BSs are fixed, thus the additional precoder plays an incremental part in the multi-BS JT operations. An iterative algorithm is designed to jointly optimize the sub-stream precoder and sub-stream power allocation for each additional BS in the proposed sequential and incremental optimization scheme. Simulations show that, under the practical backhaul link conditions, our scheme significantly outperforms the autonomous global precoding (AGP) scheme in terms of BER performance.

Index Terms—Network MIMO, Joint Transmission, Precoding, Imperfect Backhaul.

I. INTRODUCTION

Recently, there have been considerable interests in network multiple-input multiple-output (MIMO) systems [1], where multiple geographically distributed multi-antenna base stations (BSs) cooperate with each other to transmit data to users. In [2], it is shown that network MIMO can be employed to mitigate co-channel interference and to exploit macro-diversity. Motivated by these works, downlink network MIMO technologies have been adopted by 4G mobile communication standards, such as the 3rd Generation Partnership Project (3GPP) Long Term Evolution-Advanced (LTE-A) networks [3].

The cooperating strategies for network MIMO systems can be generally divided into two categories, i.e., coordinated beamforming (CB) and joint transmission (JT). When the CB strategy is employed, the cooperating BSs share channel

state information (CSI) in various forms, and each BS only transmits data to its own served users, while for the JT strategy, both CSI and user data should be shared by all cooperating BSs, and thus each user receives data from multiple BSs. Many current research works focus on CB network MIMO schemes [4], [5], [6], [7]. However, the performance of CB strategy is generally interference-limited due to lack of abundant spatial-domain degrees of freedom for perfect inter-BS interference coordination in practical systems [1]. On the other hand, the JT strategy takes a more aggressive approach to cope with the interference problem by transforming the interference from neighbor BSs into useful signals. Usually, the mathematical form of the JT scheme bears a close resemblance to conventional MIMO systems except for its distributed structure [8]. From uplink-downlink duality theory, the capacity region of the downlink JT network MIMO systems can be computed from its dual uplink [9] with the same sum power constraint. These results were later generalized to accommodate the per-antenna power constraint [10] by showing that the per-antenna downlink transmitter optimization problem can be transformed into a dual uplink problem with an uncertain noise. It should be noted that most capacity duality results are based on non-linear signal processing at the BS side, such as the dirty paper coding [11], which is computationally demanding for precoding across multiple BSs. This has motivated research in linear precoding for JT, such as zero-forcing (ZF) precoders [12], which are much more easy-to-implement compared with the DPC precoder. Moreover, when user equipment (UE) is equipped with multiple antennas, the distributed transceiver design [13], i.e., designing the precoder with UE's receiver structure taken into account, should also be considered for JT. Another relevant issue regarding JT is the imperfect backhaul links [14]. In practice, cooperating BSs are connected through imperfect links with finite capacity, unpredictable latency, and limited connectivity. For example, the latency of practical backhaul links such as the copper and wireless interface varies from several milliseconds to tens of milliseconds depending on technology/standard. Besides, when the backhaul communication is based on a generic IP network, the backhaul latency also depends on the number of routers between two cooperative BSs and the topology of the network, e.g., star, ring, tree, mesh, etc. Furthermore, congestion in the routers causes an extra delay typically of several milliseconds [15]. It should be noted that limited capacity is another important backhaul issue [16]. Most of the current cellular backhaul networks are designed for handover functions, which are not suited for

Copyright (c) 2012 IEEE. Personal use of this material is permitted. However, permission to use this material for any other purposes must be obtained from the IEEE by sending a request to pubs-permissions@ieee.org.

Ming Ding, Jun Zou, Hanwen Luo and Wen Chen are with the Dept. of Electronic Engineering, Shanghai Jiaotong University, Shanghai, P. R. China. (E-mail: {dm2007, zoujun, hwluo, wenchen}@sjtu.edu.cn).

Ming Ding and Zeng Yang are with Sharp Laboratories of China Co., Ltd. (E-mail: {ming.ding, zeng.yang}@cn.sharp-world.com).

This work is sponsored by Sharp Laboratories of China Co., Ltd.

data exchange in large amount [3]. Constraints from lower capacity/higher latency backhaul communication in coordinated multi-point (CoMP) operations were studied in the 3GPP LTE-A meetings [17], [18]. Due to the immature status of the study, remote radio head (RRH) or remote radio equipment (RRE) based centralized BS and fiber based backhaul [19] were assumed for the JT as a starting point of the working order for the imperfect backhaul issue [20]. Although the current centralized network structure and fiber based backhaul will not pose serious problems for existing JT schemes, for future JT operations, the impact of imperfect backhaul should be carefully investigated [21]. Up to now, theoretical performance bounds for JT network MIMO with unreliable backhaul links among the cooperating BSs are unknown yet [1]. Finally, it should also be noted that imperfect CSI fed back by the UE is a common assumption in practical frequency division duplexing (FDD) systems such as the 3GPP LTE-A system, where the downlink CSI cannot be inferred from the uplink CSI. For imperfect CSI feedback in a practical system, implicit CSI feedback, i.e., feedback of precoder recommendation by UEs [3], is much more preferred than the explicit CSI feedback, i.e., feedback of the channel matrix, due to feedback overhead considerations. In this paper, we consider the implicit CSI feedback, which has been widely adopted by practical systems such as the 3GPP LTE-A system [3].

In this paper we investigate the precoder design for downlink JT network MIMO systems with imperfect backhaul links, i.e., finite capacity, unpredictable latency, and limited connectivity. In particular, we focus on network impairments incurred by backhaul delays. For JT operations, both the transmission data and the CSI must be available at the actual transmission BSs before the transmission starts; otherwise the JT cannot be operated as it was supposed to be. In a multi-BS JT network where one serving BS and several helper BSs constitute a JT set, we assume that UE's data will always arrive at the serving BS from higher-layer entities in a timely and error-free manner, then the serving BS shares the data with the helper BSs by means of imperfect backhaul communications. Here, the serving BS does not necessarily mean the BS with the strongest signal level at the UE, the typical event of which occurs during inter-BS handover process. According to [3], the serving BS is defined as the BS sending downlink control signalings, e.g., downlink scheduling information, to the UE. In the sense of downlink control signaling connection, the helper BSs are not equal partners with the serving BS because they only provide data transmissions to the UE. Besides, regarding the CSI feedback, we assume that the UE reports the precoder recommendation information either to each individual BS in the JT set or to the serving BS which in turn exchanges this information among helper BSs over backhaul links. Whether both the transmission data and the CSI arrive at a certain helper BS before the JT scheduled to be performed or not is a probabilistic event because of the non-deterministic delay, which has been shown to conform to a shifted gamma distribution in [22]. If a helper BS fails to obtain both the transmission data and the CSI in time, then it has to quit the JT operations. Thereby, whether a helper BS can participate in JT or not is also a probabilistic event. Since

the average bit error rate (BER) of the system is generally dominated by the sub-stream with the maximum mean square error (MSE) [23], we propose a precoding scheme to minimize the maximum of the sub-stream MSEs. In the proposed scheme, we first optimize the precoder at the serving BS, and then sequentially optimize the precoders of helper BSs in the JT set according to the descending order of their probabilities of participating in JT. The BS-wise sequential optimization process can improve the system performance when some helper BSs have to temporarily quit the JT operations because of poor instant backhaul conditions. Besides, the precoder of an additional BS is derived in an incremental way, i.e., the sequentially optimized precoders of previous BSs are fixed, thus the additional precoder plays an incremental part in the multi-BS JT operations. Because the BS precoders are generated sequentially and incrementally, our proposed scheme will be referred to as the sequential and incremental precoding (SIP) scheme hereafter. An iterative algorithm is designed to jointly optimize the sub-stream precoder and power allocation (PA) for each additional BS in the SIP scheme. Simulation results show that our scheme can achieve considerable gains in terms of BER performance compared with a variation of global precoding (GP) scheme, i.e., autonomous global precoding (AGP) scheme, under the practical backhaul link conditions.

There are several benefits offered by our scheme. First, it offers flexibility to the JT network MIMO since the helper BSs can adaptively decide whether or not to join JT according to their own situation. Such JT scheme enables the network MIMO to adaptively switch among single-BS transmission (ST), partial JT and full JT without inter-BS signaling. Here partial JT refers to the transmission from a subset of BSs within the JT set. Second, the related CSI feedback scheme can easily fit into the current 3GPP LTE-A per-BS feedback framework [3], i.e., the feedback operation is performed on a per-BS basis, which facilitates the feedback design. Third, the complexity on the UE side to select a preferred precoder from a codebook is low. Instead of searching for the precoder through a large codebook as done in the conventional GP scheme, the precoder for each BS is obtained from a small per-BS based codebook. .

The rest of the paper is organized as follows. Section II presents the system model and briefly describes backhaul impairments. Section III discusses the GP and Autonomous GP (AGP) scheme. Section IV proposes the sequential and incremental precoder design and its extension to multi-BS JT network MIMO systems. The paper is completed with simulation results and conclusions in sections V and VI, respectively.

Notations: $(\cdot)^T$, $(\cdot)^*$, $(\cdot)^H$ and $\text{tr}\{\cdot\}$ stand for the transpose, conjugate, conjugate transpose, and trace of a matrix, respectively. $\mathbf{A}_{i,j}$, $\mathbf{A}_{i,:}$, and $\mathbf{A}_{:,j}$ denote the (i, j) -th entry, i -th row, and j -th column of matrix \mathbf{A} , respectively. $\text{diag}\{\mathbf{A}_k\}$ denotes a block-diagonal matrix with the k -th diagonal block given by \mathbf{A}_k . \mathbf{I}_N stands for an $N \times N$ identity matrix. $|\mathbf{a}|$ denotes the Euclidean norm of a vector \mathbf{a} . $\mathbb{E}\{\cdot\}$ and $\text{Re}\{\cdot\}$ denote expectation operator and the real part of a complex value, respectively. Finally, we define $(a)^+ = \max(0, a)$.

II. SYSTEM MODEL

In this section, we address the system model and briefly discuss backhaul impairments. We consider a multi-cell wireless network consisting of B adjacent BSs, where each BS is equipped with N_T antennas. A cell edge UE with N_R antennas is served by one serving BS, and the other $B-1$ BSs are helper BSs which adaptively provide service to the UE depending on the backhaul conditions. In practice, the candidates of helper BSs can be decided either by UE based on received reference signal strength of nearby BSs, or by the serving BS based on wideband CSI reported by UE. The selection algorithm to decide the helper BSs can be found in [24] and [25]. Here, we assume $B-1$ helper BSs have already been selected based on some existing BS selection schemes. Moreover, in practical scenarios, values of B are relatively small, usually not larger than 4 [26].

A. The JT Networks with Two BSs

Our basic idea to optimize the precoders for the B BSs in the JT set to derive per-BS precoders one by one in a sequential and incremental manner. Hence, the most basic scenario is a JT network with only two BSs. A two-BS JT network ($B=2$) is shown in Fig. 1, which serves as an instructive example to formulate the key problem of our concern. An N_R -antenna cell edge UE is associated with a serving BS₁ and the transmission is assisted by a helper BS₂. Note that the results from this model will later be extended to a more general model with multiple BSs in the JT set.

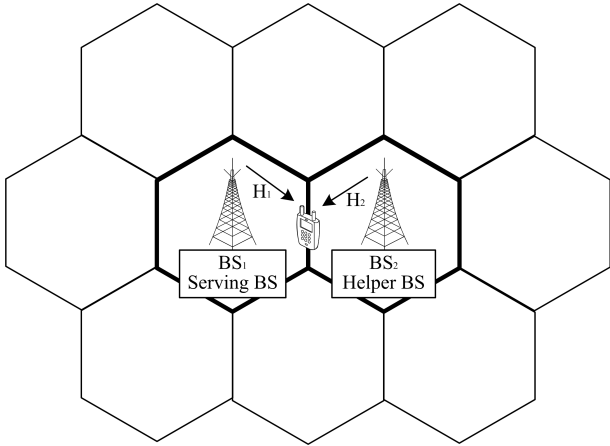


Fig. 1. Illustration of a two-BS JT network.

In Fig. 1, the base-band channel matrix between the b -th BS and the UE is denoted as $\mathbf{H}_b \in \mathbb{C}^{N_R \times N_T}$. The UE reports the precoder recommendation information either to each individual BS in the JT set or to the serving BS which in turn exchanges this information among helper BSs over backhaul links. Let $\mathbf{W}_b \in \mathbb{C}^{N_T \times L}$ be the local precoding matrix of the b -th BS, where L is the number of independent data sub-streams for the UE. In addition, \mathbf{W}_b is subjected to a per-BS power constraint $\text{tr}\{\mathbf{W}_b^H \mathbf{W}_b\} \leq P$, where P is the maximum transmission power at each BS. Then the signal received at the UE can be described by

$$\mathbf{y} = [\mathbf{H}_1, \mathbf{H}_2] \begin{bmatrix} \mathbf{W}_1 \\ \mathbf{W}_2 \end{bmatrix} \mathbf{x} + \mathbf{n}, \quad (1)$$

where $\mathbf{x} = [x_1, x_2, \dots, x_L]^T$ is the transmission data vector with $\mathbb{E}\{\mathbf{x}\mathbf{x}^H\} = \mathbf{I}_L$ and \mathbf{n} is the noise vector with $\mathbb{E}\{\mathbf{n}\mathbf{n}^H\} = \mathbf{R}_n$. Note that the interference from BSs outside of the interested JT set is incorporated into \mathbf{n} . Assume that the interference is white-colored [27], then \mathbf{R}_n can be simplified to $\mathbf{R}_n = N_0 \mathbf{I}_{N_R}$.

Suppose that a linear receiver $\mathbf{F} \in \mathbb{C}^{L \times N_R}$ is employed at the UE to detect \mathbf{x} . Then the MSE of the i -th ($i \in \{1, 2, \dots, L\}$) detected sub-stream can be represented by

$$M_i = \mathbb{E}\left\{|\mathbf{F}_{i,:} \mathbf{y} - x_i|^2\right\}. \quad (2)$$

In general, the average BER of the system is dominated by the sub-stream with the maximum MSE [23]. Therefore, we want to jointly design \mathbf{W}_1 , \mathbf{W}_2 and \mathbf{F} to minimize the maximum of the sub-stream MSEs. This MIN-MAX-MSE problem is formulated as

$$\begin{aligned} \min_{\mathbf{F}, \mathbf{W}_1, \mathbf{W}_2} \quad & \max\{M_i | i \in \{1, 2, \dots, L\}\}, \\ \text{s.t.} \quad & \text{tr}\{\mathbf{W}_b^H \mathbf{W}_b\} \leq P, \forall b = 1, 2. \end{aligned} \quad (3)$$

B. Modeling of Imperfect Backhaul

For full JT operations, the transmission data vector \mathbf{x} needs to be available at the actual transmission points before the transmission starts. We assume that UE's data will always arrive at the serving BS from higher-layer entities in a timely and error-free manner. Then the serving BS shares the data with the helper BSs by means of imperfect backhaul communications.

In this paper, we are mainly concerned with the impact of BS backhaul latency on system performance. In practice, backhaul links can be generally classified into three categories according to the physical media, i.e. optical fiber, copper (ADSL, ATM, VDSL, etc.) and wireless interface. The typical latency of optical fiber is below 1 ms, which can be neglected since the usual delay of channel state information (CSI) exchange and scheduling in cooperative MIMO systems is approximately 10 ms [15]. However, the latency of copper and wireless interface backhaul links varies from several milliseconds to tens milliseconds depending on technology/standard. Besides, when the backhaul communication is based on a generic IP network, the backhaul latency also depends on the number of routers between two cooperative BSs and the topology of the network, e.g., star, ring, tree, mesh, etc. Furthermore, congestion in the routers causes an extra delay typically of several milliseconds [15].

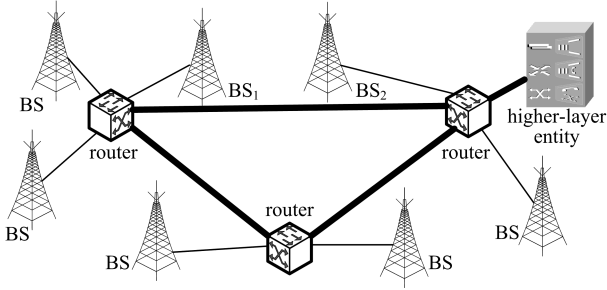


Fig. 2. Illustration of a realistic BS backhaul network.

Fig. 2 illustrates an example of a practical BS backhaul network, which combines the ring and tree topologies. If BS_1 wants to share data with BS_2 , it has to set up a backhaul link over several routers. It should be noted that limited capacity is another important backhaul issue [16]. Most of the current cellular backhaul networks are designed for handover functions, which are not suited for data exchange in large amount [3]. However, we assume capacity is adequate for backhaul communication throughout this paper.

According to [28], the maximum delay for normal backhaul links is around 20 ms and the typical average delay is expected to be within 10 ms. More detailed description of the backhaul latency model can be found in [22]. The backhaul delay conforms to a shifted gamma distribution [22], and its probability density function (PDF) can be represented by

$$f(t) = \frac{\left(\frac{t-t_0}{\alpha}\right)^{\beta-1} \exp\left\{-\frac{(t-t_0)}{\alpha}\right\}}{\alpha\Gamma(\beta)}, \quad (4)$$

where α , β and t_0 are the scale, shape and shift parameter, respectively, and $\Gamma(\cdot)$ denotes the gamma function. According to [22], the typical values are $\alpha = 1$, $\beta = 2.5$ and $t_0 = 7.5$ ms. The corresponding PDF curve is plotted in Fig. 3 for illustration purpose.

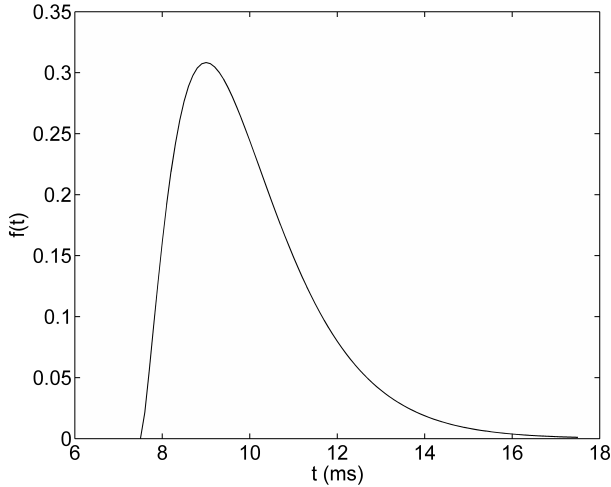


Fig. 3. Shifted gamma distribution of the backhaul delay.

In every transmission slot, the b -th ($b \in \{2, 3, \dots, B\}$) helper BS joins JT with probability p_b , which is determined by the condition of the backhaul link between the serving BS and the b -th helper BS. In the following, p_b will be referred to

as participation probability, which can be computed from (4). Suppose that the JT operation is scheduled to be performed at a critical time T after the serving cell pushes the UE's data into the backhaul network. Then p_b can be calculated as

$$p_b = \int_0^T f(t) dt = \frac{\gamma\left(\beta, \frac{T-t_0}{\alpha}\right)}{\Gamma(\beta)}, \quad (5)$$

where $\gamma(\cdot, \cdot)$ is the lower incomplete gamma function [29]. In practice, T will take a reasonably small value to avoid performance degradation caused by outdated CSI. For instance, if $T = 10$ ms, $p_b \approx 0.58$, and if $T = 11$ ms, $p_b \approx 0.78$. Furthermore, if congestion occurs in the routers, $f(t)$ will suffer from additional shift, i.e., t_0 will take large values. For instance, let $t_0 = 8.5$, then if $T = 10$ ms, $p_b \approx 0.3$, and if $T = 11$ ms, $p_b \approx 0.58$.

III. ADVANCES AND DRAWBACKS OF THE EXISTING SCHEMES

In this section, we discuss the advances and drawbacks of the existing schemes, where different aspects such as system performance, required CSI feedback, and limited backhaul connectivity are carefully examined.

A. The Global Precoding Scheme

The optimal precoding strategy for the full JT problem (3) is the global precoding (GP), i.e., to view the distributed antenna ports from BSs in the JT set as a giant multiple-antenna system and generalize the well-studied point-to-point MIMO transmission strategies to JT across multiple BSs [1]. However, the difficulty lies in how to maintain the distributed per-BS power constraints while extending the point-to-point MIMO schemes to network MIMO ones. To our best knowledge, the MIN-MAX-MSE problem is still an open problem for the linear precoding design for JT network MIMO with distributed per-BS power constraints.

Hence, a sum power constraint is instead assumed for the GP to yield a lower bound for the MSE performance [1]. To formulate GP, rewrite (1) as

$$\mathbf{y} = \mathbf{H}\mathbf{W}\mathbf{x} + \mathbf{n}, \quad (6)$$

where \mathbf{H} and \mathbf{W} denote the global channel matrix $[\mathbf{H}_1, \mathbf{H}_2]$ and global precoder $[\mathbf{W}_1^T, \mathbf{W}_2^T]^T$, respectively. The MIN-MAX-MSE problem for GP can be re-formulated from (3) as

$$\begin{aligned} \min_{\mathbf{F}, \mathbf{W}} \quad & \max \{M_i | i \in \{1, 2, \dots, L\}\}, \\ \text{s.t.} \quad & \text{tr}\{\mathbf{W}^H \mathbf{W}\} \leq 2P. \end{aligned} \quad (7)$$

Let $\mathbf{R}_H = \mathbf{H}^H \mathbf{R}_n^{-1} \mathbf{H}$, and its eigenvalue decomposition be

$$\mathbf{R}_H = \mathbf{V} \mathbf{\Lambda} \mathbf{V}^H, \quad (8)$$

where $\mathbf{V} \in \mathbb{C}^{2N_T \times 2N_T}$ is a unitary matrix and $\mathbf{\Lambda} = \text{diag}\{\lambda_i\}$ is a semi-definite diagonal matrix, with diagonal entries λ_i 's being the eigenvalues of \mathbf{R}_H . Then the optimal solution for problem (7) is achieved by the joint linear transceiver design

[30]. The optimal receiver should take the form of the Wiener filter [31] shown as

$$\mathbf{F}^{\text{opt}} = \mathbf{H}_{\text{eq}}^{\text{H}} (\mathbf{H}_{\text{eq}} \mathbf{H}_{\text{eq}}^{\text{H}} + \mathbf{R}_n)^{-1}, \quad (9)$$

where $\mathbf{H}_{\text{eq}} = \mathbf{H}\mathbf{W}$ denotes the equivalent channel. Note that the Wiener filter has been proved to be the optimum linear receiver in the sense that it minimizes each of the sub-stream MSEs [30]. And the optimal transmit precoding matrix \mathbf{W}^{opt} should be

$$\mathbf{W}^{\text{opt}} = \tilde{\mathbf{W}}\mathbf{Q}^{\text{H}} = \tilde{\mathbf{V}}\Sigma\mathbf{Q}^{\text{H}}, \quad (10)$$

where $\tilde{\mathbf{W}} = \tilde{\mathbf{V}}\Sigma$ and the column of $\tilde{\mathbf{V}} \in \mathbb{C}^{2N_{\text{T}} \times L}$ consists of the eigenvectors of \mathbf{R}_{H} corresponding to the L largest eigenvalues in increasing order. The power loading matrix $\Sigma = \text{diag}\{\sigma_i\}$. The σ_i s are tuned so that the sum MSE with respect to $\tilde{\mathbf{W}}$ is minimized. In [30], it is proved that the optimal σ_i s can be obtained by the famous water-filling power allocation (PA) [31]

$$\sigma_i = \sqrt{\left(\mu^{-1/2}\lambda_i^{-1/2} - \lambda_i^{-1}\right)^+}, \quad (11)$$

where $\mu^{-1/2}$ is the water-level chosen to satisfy the power constraint with equality.

After minimizing the sum MSE by $\tilde{\mathbf{W}}$, a rotation operation is applied on it. In (10), $\mathbf{Q} \in \mathbb{C}^{L \times L}$ is a unitary rotation matrix such that all sub-stream MSEs are equal. Thereby, the minimized sum MSE is equally divided for each sub-stream, leading to a minimized MSE \hat{M} for the maximum of the sub-stream MSEs for the problem (7), which can be concisely expressed as [30],

$$\begin{aligned} \hat{M} &= \max\{M_i\} \\ &= \frac{1}{L} \text{tr} \left\{ \left(\mathbf{I}_L + (\mathbf{W}^{\text{opt}})^{\text{H}} \mathbf{R}_{\text{H}} \mathbf{W}^{\text{opt}} \right)^{-1} \right\}. \end{aligned} \quad (12)$$

Though the closed-form expression for \mathbf{Q} does not exist, efficient algorithms to compute \mathbf{Q} can be found in [32]. Note that (12) is a lower bound solution for the original problem (3) since inter-BS PA implied by (10) is usually not the feasible solutions of (3). Besides, other practical issues such as limited backhaul and feedback overhead also compromise the performance of GP.

B. The Autonomous Global Precoding Scheme

In practice, full JT, which is assumed by GP, is not always feasible due to backhaul limitations, such as overtime delay leading to incomplete or outdated data at the transmission points. Moreover, it is preferable for practical systems to have distributed schedulers due to considerations of low complexity and low cost, thereby some local scheduling constraints in helper BSs may also force them to temporarily leave the JT set and thus break the full JT operation. Hence, it is desirable to design a flexible JT scheme, in which the serving BS makes the JT scheduling decision and informs the helper BSs, then the helper BSs can adaptively join or quit the upcoming JT operation according to their instantaneous states. If all the

helper BSs are temporarily unavailable for JT, the system should be able to fall back to single-BS transmission (ST) smoothly. But this gives rise to a feedback problem. The transmission assumption, based on which the recommended precoder is computed and fed back by the UE, may be inconsistent with the one when the transmission eventually takes place. Consequently, the previously fed-back precoder mismatches the transmission channel, causing performance degradation. This problem is not uncommon, especially in 3GPP LTE-A systems [3]. A straightforward solution to the above problem is to require the UE to feedback multiple precoder recommendations under different transmission assumptions. For example, in Fig. 1 the UE can feedback two precoders, one for JT and another for ST.

However, aside from the issue of necessary inter-BS signaling for switching between JT and ST precoders, additional feedback overhead incurred from multiple precoders will become very large, since the number of transmission assumptions can be as many as 2^{B-1} . To avoid increasing the feedback overhead, another approach would be to instruct the UE to feedback the global precoder \mathbf{W}^{opt} only. If any helper BSs are not ready for JT, they will mute themselves during the data transmission to keep the interference low, which is called dynamic point muting in the LTE-A system [33]. We assume that each helper BS is unaware of the states of other helper BSs, and thus they should stick to their respective sub-block parts of \mathbf{W}^{opt} . Such scheme is hereafter referred to as autonomous global precoding (AGP) and the corresponding precoder $\mathbf{W}_b^{\text{opt}}$ for the b -th BS can be expressed as (13) shown at the top of the next page. In (13), $\mathbf{W}_{i,:}$ denotes the i -th row of \mathbf{W} , thus $\left[\mathbf{W}_{(b-1)N_{\text{T}}+1,:}^{\text{opt T}}, \dots, \mathbf{W}_{bN_{\text{T}},:}^{\text{opt T}} \right]^{\text{T}}$ represents the sub-block part of \mathbf{W}^{opt} spanning from the $((b-1)N_{\text{T}}+1)$ -th row to the (bN_{T}) -th row of \mathbf{W}^{opt} . Since \mathbf{W}^{opt} is optimized under the assumption of full JT, its sub-block part shown in (13) may not match individual \mathbf{H}_b very well, which may result in large performance degradation when the system falls back to ST or partial JT. Therefore, in this paper we propose a flexible and adaptive precoding scheme to alleviate the problem.

IV. THE PROPOSED SEQUENTIAL AND INCREMENTAL PRECODING SCHEME

We propose a sequential and incremental precoding (SIP) scheme which is flexible and achieves satisfactory performance especially for partial JT. In the proposed SIP scheme, the precoder optimization is performed for each helper BS according to the descending order of participation probabilities with the precoders of previous BSs fixed. To facilitate the optimization, we require that the participation probabilities be determined by the serving BS based on (5), and the descending order of the participation probabilities be notified to the UE before it derives the precoders. We first investigate the precoder design for a two-BS JT network. The results are then extended to a multi-BS JT network.

A. Precoder Design for the Two-BS JT Network

We address the optimization problem (3) for the two-BS JT network introduced in Section II. We decouple problem (3)

$$\mathbf{W}_b^{\text{opt}} = \begin{cases} \mathbf{0}, & \text{the } b\text{-th BS is absent from JT,} \\ \left[\mathbf{W}_{(b-1)N_T+1,:}^{\text{opt T}}, \dots, \mathbf{W}_{bN_T,:}^{\text{opt T}} \right]^T, & \text{otherwise,} \end{cases} \quad (13)$$

into two sequential steps.

In the first step, we optimize the precoder at the serving BS to ensure the service quality when the system falls back to ST. The problem can be formulated as

$$\begin{aligned} \min_{\mathbf{F}, \mathbf{W}_1} \quad & \max \{M_i | i \in \{1, 2, \dots, L\}\}, \\ \text{s.t.} \quad & \text{tr} \{ \mathbf{W}_1^H \mathbf{W}_1 \} \leq P. \end{aligned} \quad (14)$$

Note that the above problem is essentially the same as the problem (7) except for the substitution of \mathbf{W} with \mathbf{W}_1 and the maximum power. Therefore, the optimal solution for (14) can be readily obtained as

$$\mathbf{W}_1^{\text{opt}} = \tilde{\mathbf{V}}_1 \boldsymbol{\Sigma}_1 \mathbf{Q}_1^H, \quad (15)$$

where $\tilde{\mathbf{V}}_1$, $\boldsymbol{\Sigma}_1 = \text{diag} \{ \sigma_{1,i} \}$ and \mathbf{Q}_1 are derived using the same method as their counterparts in (10) without subscripts.

In the second step, we proceed to optimize the performance of the two-BS JT with \mathbf{W}_1 fixed as $\mathbf{W}_1 = \mathbf{W}_1^{\text{opt}}$. This problem can be formulated as

$$\begin{aligned} \min_{\mathbf{F}, \mathbf{W}_2} \quad & \max \{M_i | i \in \{1, 2, \dots, L\}\}, \\ \text{s.t.} \quad & \text{tr} \{ \mathbf{W}_2^H \mathbf{W}_2 \} \leq P. \end{aligned} \quad (16)$$

Problem (16) can be considered as a conditional optimization problem for \mathbf{W}_2 with the previously derived $\mathbf{W}_1^{\text{opt}}$ fixed. Direct optimization of problem (16) is not an easy task since the aforementioned approach of minimizing the sum MSE followed by unitary rotation for problem (7) and (14) cannot be applied here. Hence we resort to an iterative method to minimize the $\max \{M_i\}$.

Suppose that we have a precoding matrix $\mathbf{W}_2^{(n)}$ in the n -th iteration. Then the equivalent channel can be written as

$$\mathbf{H}_{\text{eq}}^{(n)} = \mathbf{H}_1 \mathbf{W}_1^{\text{opt}} + \mathbf{H}_2 \mathbf{W}_2^{(n)}. \quad (17)$$

Similar to (9), at UE side the Wiener filter is also employed in order to minimize the MSE, which is described as

$$\mathbf{F}^{\text{opt},(n)} = \mathbf{H}_{\text{eq}}^{(n)H} \left(\mathbf{H}_{\text{eq}}^{(n)} \mathbf{H}_{\text{eq}}^{(n)H} + \mathbf{R}_n \right)^{-1}. \quad (18)$$

Then the MSE of the i -th sub-stream can be written as

$$M_i^{(n)} = \mathbb{E} \left\{ \left| \mathbf{F}_{i,:}^{\text{opt},(n)} \left(\mathbf{H}_{\text{eq}}^{(n)} \mathbf{x} + \mathbf{n} \right) - x_i \right|^2 \right\}. \quad (19)$$

Denote the sub-stream index associated with the maximum sub-stream MSE as

$$j(n) = \arg \max_i \{M_i^{(n)}\}. \quad (20)$$

Next we update $\left(\mathbf{W}_2^{(n+1)} \right)_{:,j(n)}$ subject to a sub-stream power constraint $P_{2,j(n)}^{(n+1)}$ with fixed $\mathbf{F}^{\text{opt},(n)}$ such that $M_{j(n)}^{(n+1)}$

is minimized. Denote $\mathbf{g} = \left(\mathbf{W}_2^{(n+1)} \right)_{:,j(n)}$ for convenience. Then the problem (16) can be formulated as

$$\begin{aligned} \min_{\mathbf{g}} \quad & M_{j(n)}^{(n+1)}, \\ \text{s.t.} \quad & \text{tr} \{ \mathbf{g}^H \mathbf{g} \} \leq P_{2,j(n)}^{(n+1)}, \end{aligned} \quad (21)$$

where $M_{j(n)}^{(n+1)}$ can be represented in detail as (22) shown at the top of the next page. We further fix $\left(\mathbf{W}_2^{(n+1)} \right)_{:,i}$ for $i \neq j(n)$. Omitting the irrelevant terms in (22) for simplicity, we get

$$\begin{aligned} \tilde{M}_{j(n)}^{(n+1)} = & \left| \mathbf{F}_{j(n),:}^{\text{opt},(n)} \left(\mathbf{H}_1 \left(\mathbf{W}_1^{\text{opt}} \right)_{:,j(n)} + \mathbf{H}_2 \mathbf{g} \right) \right|^2 \\ & - 2 \text{Re} \left\{ \mathbf{F}_{j(n),:}^{\text{opt},(n)} \left(\mathbf{H}_1 \left(\mathbf{W}_1^{\text{opt}} \right)_{:,j(n)} + \mathbf{H}_2 \mathbf{g} \right) \right\}. \end{aligned} \quad (23)$$

Hence, problem (21) is equivalent to the following problem

$$\begin{aligned} \min_{\mathbf{g}} \quad & \tilde{M}_{j(n)}^{(n+1)}, \\ \text{s.t.} \quad & \text{tr} \{ \mathbf{g}^H \mathbf{g} \} \leq P_{2,j(n)}^{(n+1)}. \end{aligned} \quad (24)$$

It is easy to verify that the problem (24) is convex. Thus, we can obtain the optimal \mathbf{g} from the KKT conditions [34]. The Lagrangian function of (24) is given by

$$\mathcal{L}(\mathbf{g}, \eta) = \tilde{M}_{j(n)}^{(n+1)} + \eta \left(\text{tr} \{ \mathbf{g}^H \mathbf{g} \} - P_{2,j(n)}^{(n+1)} \right), \quad (25)$$

where $\eta \geq 0$ is the Lagrangian multiplier. Taking its derivative with respect to \mathbf{g}^* , we have

$$\begin{aligned} \frac{\partial \mathcal{L}}{\partial \mathbf{g}^*} = & \mathbf{H}_2^H \left(\mathbf{F}_{j(n),:}^{\text{opt},(n)} \right)^H \mathbf{F}_{j(n),:}^{\text{opt},(n)} \left(\mathbf{H}_1 \left(\mathbf{W}_1^{\text{opt}} \right)_{:,j(n)} + \mathbf{H}_2 \mathbf{g} \right) \\ & - \mathbf{H}_2^H \left(\mathbf{F}_{j(n),:}^{\text{opt},(n)} \right)^H + \eta \mathbf{g}. \end{aligned} \quad (26)$$

The KKT conditions are as follows

$$\begin{cases} \frac{\partial \mathcal{L}}{\partial \mathbf{g}^*} = 0, & \text{(a)} \\ \eta \left(\text{tr} \{ \mathbf{g}^H \mathbf{g} \} - P_{2,j(n)}^{(n+1)} \right) = 0, & \text{(b)} \\ \text{tr} \{ \mathbf{g}^H \mathbf{g} \} \leq P_{2,j(n)}^{(n+1)}. & \text{(c)} \end{cases} \quad (27)$$

From (27), the closed-form expression for \mathbf{g} can be derived as

$$\begin{aligned} \mathbf{g} = & \left(\mathbf{H}_2^H \left(\mathbf{F}_{j(n),:}^{\text{opt},(n)} \right)^H \mathbf{F}_{j(n),:}^{\text{opt},(n)} \mathbf{H}_2 + \eta \mathbf{I} \right)^{-1} \\ & \times \mathbf{H}_2^H \left(\left(\mathbf{F}_{j(n),:}^{\text{opt},(n)} \right)^H - \left(\mathbf{F}_{j(n),:}^{\text{opt},(n)} \right)^H \mathbf{F}_{j(n),:}^{\text{opt},(n)} \mathbf{H}_1 \left(\mathbf{W}_1^{\text{opt}} \right)_{:,j(n)} \right), \end{aligned} \quad (28)$$

where η should be chosen such that (27.b) and (27.c) are satisfied.

The remaining problem is the power allocation (PA) strategy for $P_{2,j(n)}^{(n+1)}$. As shown by [30], the optimal solution for the MIN-MAX-MSE problem (7) is achieved when the sub-stream

$$\begin{aligned}
M_{j(n)}^{(n+1)} &= \mathbb{E} \left\{ \left| \mathbf{F}_{j(n),:}^{\text{opt},(n)} \left(\left(\mathbf{H}_1 \mathbf{W}_1^{\text{opt}} + \mathbf{H}_2 \mathbf{W}_2^{(n+1)} \right) \mathbf{x} + \mathbf{n} \right) - x_{j(n)} \right|^2 \right\} \\
&= \sum_{i \neq j(n)} \left| \mathbf{F}_{j(n),:}^{\text{opt},(n)} \left(\mathbf{H}_1 \left(\mathbf{W}_1^{\text{opt}} \right)_{:,i} + \mathbf{H}_2 \left(\mathbf{W}_2^{(n+1)} \right)_{:,i} \right) \right|^2 \\
&\quad + \left| \mathbf{F}_{j(n),:}^{\text{opt},(n)} \left(\mathbf{H}_1 \left(\mathbf{W}_1^{\text{opt}} \right)_{:,j(n)} + \mathbf{H}_2 \mathbf{g} \right) \right|^2 \\
&\quad - 2 \text{Re} \left\{ \mathbf{F}_{j(n),:}^{\text{opt},(n)} \left(\mathbf{H}_1 \left(\mathbf{W}_1^{\text{opt}} \right)_{:,j(n)} + \mathbf{H}_2 \mathbf{g} \right) \right\} \\
&\quad + \mathbf{F}_{j(n),:}^{\text{opt},(n)} \mathbf{R}_n \left(\mathbf{F}_{j(n),:}^{\text{opt},(n)} \right)^H + N_0.
\end{aligned} \tag{22}$$

MSEs are equal. Motivated by this result, we propose to transfer a small amount of power from the sub-stream with minimum MSE to that with maximum MSE in each iteration. In such way, the maximum MSE $M_{j(n)}^{(n)}$ in the n -th iteration will decrease to $M_{j(n)}^{(n+1)}$ due to the optimized precoding vector \mathbf{g} together with additional power bonus received from the sub-stream with minimum MSE.

Let

$$k(n) = \arg \min_i \left\{ M_i^{(n)} \right\}, \tag{29}$$

we update the PA as follows

$$\begin{cases} P_{2,j(n)}^{(n+1)} = P_{2,j(n)}^{(n)} + \delta P_{2,k(n)}^{(n)}, \\ P_{2,k(n)}^{(n+1)} = P_{2,k(n)}^{(n)} \times (1 - \delta), \\ P_{2,i}^{(n+1)} = P_{2,i}^{(n)}, \end{cases} \quad \text{for } i \neq j(n), k(n), \tag{30}$$

where

$$P_{2,l}^{(n)} = \left| \left(\mathbf{W}_2^{(n)} \right)_{:,l} \right|^2, l \in \{1, 2, \dots, L\}, \tag{31}$$

and δ is the percentage of power transferred from the $k(n)$ -th sub-stream to the $j(n)$ -th sub-stream. Based on (28) and (30), $\mathbf{W}_2^{(n+1)}$ can be updated as

$$\begin{cases} \left(\mathbf{W}_2^{(n+1)} \right)_{:,j(n)} = \mathbf{g}, \\ \left(\mathbf{W}_2^{(n+1)} \right)_{:,k(n)} = \sqrt{1 - \delta} \left(\mathbf{W}_2^{(n)} \right)_{:,k(n)}, \\ \left(\mathbf{W}_2^{(n+1)} \right)_{:,i} = \left(\mathbf{W}_2^{(n)} \right)_{:,i}, \text{ for } i \neq j(n), k(n). \end{cases} \tag{32}$$

Note that the power allocation should be initialized such that $\sum_{l=1}^L P_{2,l}^{(0)} = P$ so that in the following iterations, the power constraint of $\mathbf{W}_2^{(n)}$ can always be satisfied. When the iterative algorithm converges, all sub-stream MSEs should be equal. Hence, the termination criterion can be established based on the difference between $M_{j(n)}^{(n)}$ and $M_{k(n)}^{(n)}$. The proposed precoding scheme will be referred to as the sequential and incremental precoding (SIP) scheme hereafter and is summarized in Algorithm 1.

Algorithm 1 The SIP Scheme for Two-BS JT

Step 1: Compute $\mathbf{W}_1^{\text{opt}}$ according to (15);

Step 2: Obtain $\mathbf{W}_2^{\text{opt}}$ using the following iterative algorithm,

1) Initialization:

Set $\mathbf{W}_2^{(1)} = \sqrt{\frac{P}{L}} [\mathbf{I}_L, \mathbf{0}_{L \times (N_T - L)}]^T$ and $n = 1$.

2) Iteration:

(a) Compute $\mathbf{H}_{\text{eq}}^{(n)}$ and $\mathbf{F}^{\text{opt},(n)}$ using (17) and (18), respectively;

(b) Use (28) to compute \mathbf{g} and (32) to get $\mathbf{W}_2^{(n+1)}$;

3) Termination:

The algorithm terminates either when $M_{j(n)}^{(n)}$ and $M_{k(n)}^{(n)}$

converges, i.e., $\frac{|M_{j(n)}^{(n)} - M_{k(n)}^{(n)}|}{M_{j(n)}^{(n)}} \leq \xi_{\text{th}}$ or when $n \geq N_{\text{max}}$,

where ξ_{th} is a predefined threshold and N_{max} is the maximum iteration number;

Output $\mathbf{W}_2^{\text{opt}} = \mathbf{W}_2^{(n)}$.

Else, $n = n + 1$, and go to sub-step 2).

B. Extension of the SIP Scheme

In this subsection, we generalize our proposed SIP scheme to multi-BS scenarios, where $B > 2$. Without loss of generality, the $B - 1$ helper BSs are sorted by their participation probabilities in decreasing order as: $p_2 \geq p_3 \geq \dots \geq p_B$. Then the corresponding precoders are sequentially and incrementally optimized with \mathbf{W}_2 first and \mathbf{W}_B last based on Step 2 of the proposed SIP scheme. To be more specific, \mathbf{W}_b ($b \in \{2, 3, \dots, B\}$) is optimized with fixed $\mathbf{W}_i^{\text{opt}}$ ($i \in \{1, 2, \dots, b - 1\}$) previously obtained from the SIP scheme. In addition, the equivalent channel shown in (17) now should be computed as

$$\mathbf{H}_{\text{eq}}^{(n)} = \sum_{i=1}^{b-1} \mathbf{H}_i \mathbf{W}_i^{\text{opt}} + \mathbf{H}_b \mathbf{W}_b^{(n)}. \tag{33}$$

If helper BS b joins JT, its precoder will be $\mathbf{W}_b^{\text{opt}}$. Otherwise, it mutes its transmission.

To sum up, the proposed SIP scheme can be extended to be employed in a multi-BS JT scenario and is summarized in Algorithm 2.

Algorithm 2 *The SIP Scheme for Multi-BS JT*

Step 1: Compute $\mathbf{W}_1^{\text{opt}}$ according to (15);
 Set $b = 2$;
 Step 2: Obtain $\mathbf{W}_b^{\text{opt}}$ using the following iterative algorithm,
 1) Initialization:
 Set $\mathbf{W}_b^{(1)} = \sqrt{\frac{P}{L}} [\mathbf{I}_L, \mathbf{0}_{L \times (N_T - L)}]^T$ and $n = 1$;
 2) Iteration:
 (a) Compute $\mathbf{H}_{\text{eq}}^{(n)}$ and $\mathbf{F}^{\text{opt},(n)}$ using (33) and (18), respectively;
 (b) Use (28) to compute \mathbf{g} and (32) to get $\mathbf{W}_b^{(n+1)}$;
 3) Termination:
 The algorithm terminates either when $M_{j(n)}^{(n)}$ and $M_{k(n)}^{(n)}$ converges, i.e., $\frac{|M_{j(n)}^{(n)} - M_{k(n)}^{(n)}|}{M_{j(n)}^{(n)}} \leq \xi_{\text{th}}$ or when $n \geq N_{\text{max}}$, where ξ_{th} is a predefined threshold and N_{max} is the maximum iteration number;
 Output $\mathbf{W}_b^{\text{opt}} = \mathbf{W}_b^{(n)}$;
 Else, $n = n + 1$, then go to sub-step 2).
 Step 3: If $b < B$, then $b = b + 1$, and go to Step 2
 Else, terminate the algorithm with $\mathbf{W}_b^{\text{opt}} (b \in \{1, 2, \dots, B\})$ as the per-BS precoders.

C. The SIP Scheme with Codebook Based Feedback

If a codebook, denoted as Ω , is employed as the set of precoder candidates, then UE can exhaustively search Ω , find the best precoder and feedback its index to the BS using just a few bits. In practice, codebook based feedback is commonly used in FDD systems such as the LTE-A system [3] due to low overhead costs. Here, we pursue the philosophy of sequential and incremental precoding, and propose the SIP scheme with codebook based feedback.

For \mathbf{W}_1 , the best precoder in the codebook Ω can be written as

$$\mathbf{W}_1^{\text{opt,cb}} = \arg \min_{\mathbf{W}_1^{\text{cb}} \in \Omega} \max \{M_i | i \in \{1, 2, \dots, L\}\}, \quad (34)$$

where $M_i = \mathbb{E} \left\{ \left| \mathbf{F}_{i,:}^{\text{opt}} (\mathbf{H}_1 \mathbf{W}_1^{\text{cb}} \mathbf{x} + \mathbf{n}) - x_i \right|^2 \right\}$.

For \mathbf{W}_b , we fix the previously optimized precoders and incrementally find the best precoder for \mathbf{W}_b from

$$\mathbf{W}_b^{\text{opt,cb}} = \arg \min_{\mathbf{W}_b^{\text{cb}} \in \Omega} \max \{M_i | i \in \{1, 2, \dots, L\}\}, \quad (35)$$

where $M_i = \mathbb{E} \left\{ \left| \mathbf{F}_{i,:}^{\text{opt}} (\mathbf{H}_{\text{eq}} \mathbf{x} + \mathbf{n}) - x_i \right|^2 \right\}$ and $\mathbf{H}_{\text{eq}} = \sum_{i=1}^{b-1} \mathbf{H}_i \mathbf{W}_i^{\text{opt,cb}} + \mathbf{H}_b \mathbf{W}_b^{\text{cb}}$.

In the AGP scheme, the best precoder from the global codebook Ω_{GP} can be represented as

$$\mathbf{W}^{\text{opt,cb}} = \arg \min_{\mathbf{W}^{\text{cb}} \in \Omega_{\text{GP}}} \max \{M_i | i \in \{1, 2, \dots, L\}\}, \quad (36)$$

where $M_i = \mathbb{E} \left\{ \left| \mathbf{F}_{i,:}^{\text{opt}} (\mathbf{H} \mathbf{W}^{\text{cb}} \mathbf{x} + \mathbf{n}) - x_i \right|^2 \right\}$. Then the $\mathbf{W}_b^{\text{opt,cb}}$ s of the AGP scheme can be readily obtained from (13) with \mathbf{W}^{opt} replaced by $\mathbf{W}^{\text{opt,cb}}$.

Suppose that the cardinality of Ω is 2^d , then for each BS d bits are needed to feedback $\mathbf{W}_b^{\text{opt,cb}}$ from 2^d precoder candidates. In order to make a fair comparison between the SIP and AGP schemes, the cardinality of Ω_{GP} should be 2^{Bd} , i.e., a total overhead of Bd bits are assumed for the feedback of precoders in both schemes.

V. SIMULATION RESULTS AND DISCUSSIONS

In this section, we present simulation results to compare the maximum MSE and average BER performances of the proposed SIP scheme with those of the AGP scheme. We consider a practical setup where a single multi-antenna UE with $N_{\text{R}} = 2$ or 4 is served by a multi-BS JT set with $B = 2$ or 3 and $N_{\text{T}} = 4$. Suppose that the critical time $T = 11$ ms, and t_0 for BS₂ and BS₃ are set to $t_{0,2} = 7.5$ ms and $t_{0,3} = 8.5$ ms, respectively. As explained in Section II-B, the corresponding participation probabilities for BS₂ and BS₃ can be calculated using (5) and we get $p_2 \approx 0.78$ and $p_3 \approx 0.58$. Note that the water filling PA for the AGP and SIP schemes may lead to rank adaptation, i.e. dropping sub-streams with poor channel gains. For fairness, rank adaptation should be forbidden in our simulations. Therefore, when $N_{\text{R}} = 4$ we fix $L = 4$ to prevent rank adaptation and apply equal sub-stream PA to \mathbf{W}_1 , i.e., set $\sigma_{1,i} = P/L$ in (15), whereas the power transfer shown in (30) is applied for \mathbf{W}_b s when $b \neq 1$. The water filling PA is only engaged for \mathbf{W}_1 in the case of $N_{\text{R}} = 2$, when rank adaptation rarely happens. At the UE side, we assume that the Wiener filter is always employed.

We define per-BS signal to interference plus noise ratio (SINR) by $\text{SINR} = P/N_0$. All channels are assumed to experience uncorrelated Rayleigh fading and the entries of \mathbf{H}_b are i.i.d. zero-mean circularly symmetric complex Gaussian (ZMCSCG) random variables with unit variance. The results are averaged over 10,000 independent channel realizations. As for the BER results, 1,000,000 symbols obtained from the QPSK constellation are transmitted in each channel realization for each simulated SINR point. In addition, for the proposed SIP scheme, we set the convergence threshold $\xi_{\text{th}} = 0.01$, power transfer percentage $\delta = 1\%$ and the maximum iteration number $N_{\text{max}} = 100$.

A. Convergence of SIP Scheme

Before discussing the numerical results of the system performance, we first investigate the convergence behavior of the proposed SIP scheme summarized in algorithm 1. Fig. 4 and 5 show the mean of the maximum of sub-stream MSEs versus number of iterations for $B = 2$ and $N_{\text{R}} = 2$ or 4 with different SINR. As seen from these two figures, the MSE always converges. When $N_{\text{R}} = 2$, the MSE converges typically after 20 iterations, and more iterations are needed for the case of $N_{\text{R}} = 4$. Moreover, the convergence of the SIP scheme for multi-BS JT is straightforward since the mathematical form of $\mathbf{H}_{\text{eq}}^{(n)}$ in algorithm 2 is essentially the same as that in algorithm 1. Therefore, here we omit the illustration of algorithm convergence for the case of $B = 3$.

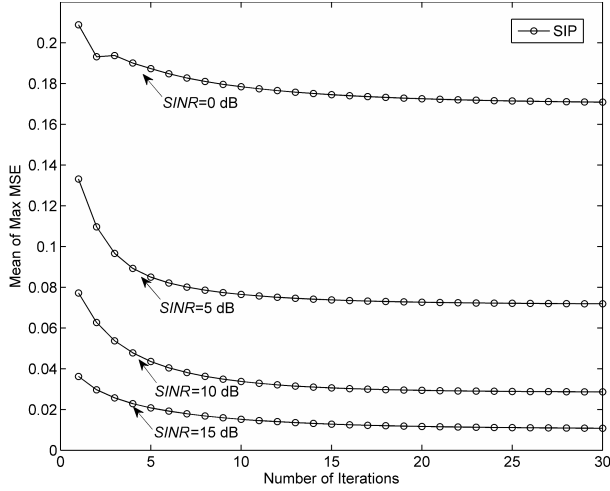


Fig. 4. Convergence of the SIP scheme for $B = 2$, $N_R = 2$ (perfect feedback).

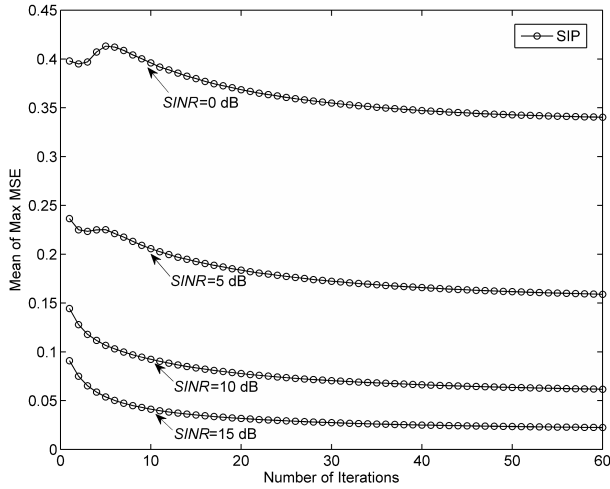


Fig. 5. Convergence of the SIP scheme for $B = 2$, $N_R = 4$ (perfect feedback).

B. Performance of the Mean of the Maximum of Sub-stream

Fig. 6 and 7 show the average performance of the maximum of sub-stream MSEs for $B = 2$ and $N_R = 2$ or 4 with different p_2 . For the case of $p_2 = 0$, the system degenerates to ST due to broken backhaul, while the case of $p_2 = 1$ corresponds to full JT with perfect backhaul. As explained in Section III and observed in Fig. 6 and 7, the precoder for the AGP scheme is optimized under the assumption of full JT, which incurs large performance degradation when the system falls back to ST or partial JT. When the practical backhaul is considered, i.e., $p_2 = 0.78$, the proposed SIP scheme offers significant performance gain and the gain is more pronounced in high SINR regimes because the sequentially and incrementally designed precoder matches the actual transmission channel better than the precoder in AGP which is optimized for full JT.

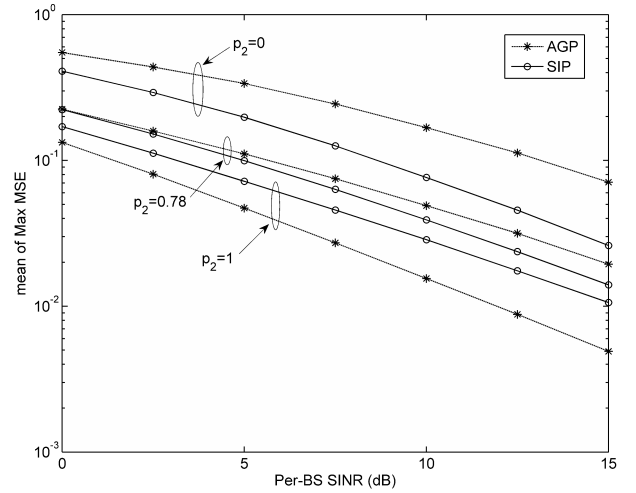


Fig. 6. Mean of the maximum of sub-stream MSEs for $B = 2$, $N_R = 2$ (perfect feedback).

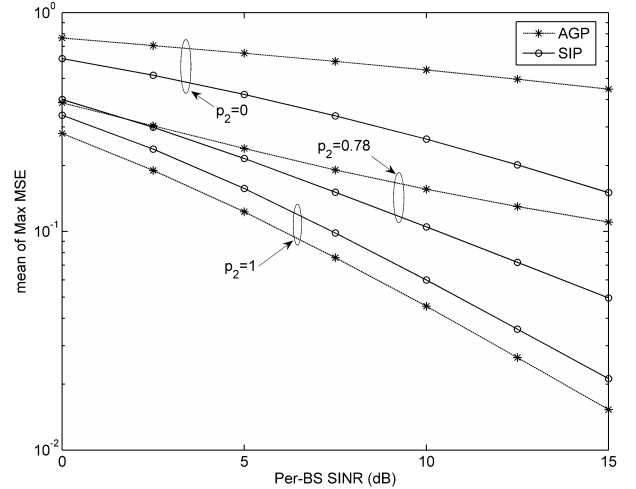


Fig. 7. Mean of the maximum of sub-stream MSEs for $B = 2$, $N_R = 4$ (perfect feedback).

C. Average BER Performance

Fig. 8 and 9 show the average BER performance for $B = 2$ and $N_R = 2$ or 4 with different p_2 . As seen from Fig. 8 and 9, our proposed SIP scheme also shows superior BER performance when $p_2 = 0.78$, especially in high SINR regimes. When $SINR = 15$ dB, compared with the AGP scheme, the proposed SIP scheme can reduce the average BER from 0.5×10^{-3} to 10^{-5} and from 10^{-2} to 3×10^{-3} for the case of $N_R = 2$ and $N_R = 4$, respectively.

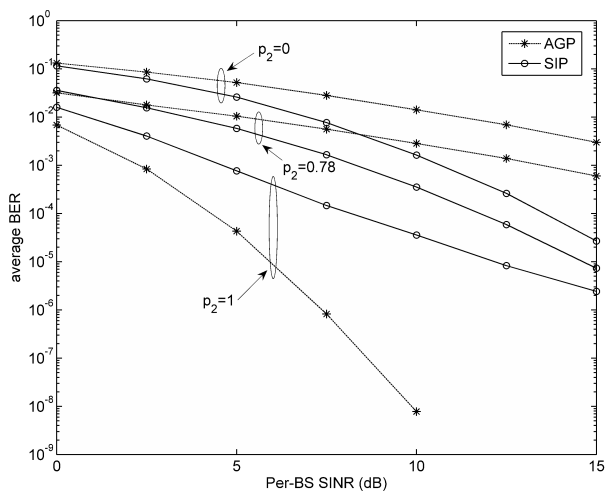


Fig. 8. Average BER for $B = 2$, $N_R = 2$ (perfect feedback).

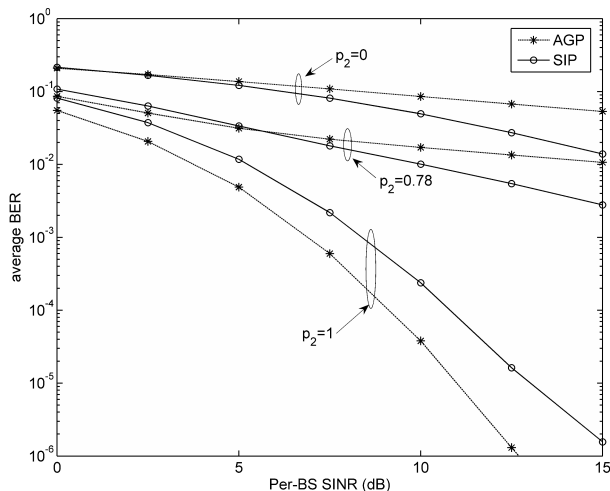


Fig. 9. Average BER for $B = 2$, $N_R = 4$ (perfect feedback).

D. Performance of the Extended SIP Scheme

For the extended case of $B = 3$, we show the average performance of the maximum of sub-stream MSEs in Fig. 10 and 11, and the corresponding BER results in Fig. 12 and 13 for $N_R = 2$ or 4 with different (p_2, p_3) . Much like what we have observed previously, when the backhaul suffers from limited connectivity, e.g., $(p_2, p_3) = (0.78, 0.58)$, the proposed SIP scheme significantly outperforms the AGP scheme in terms of average BER when SINR is high. It is very interesting to note that the SIP and AGP schemes exhibit close averaged maximum MSE curves when $(p_2, p_3) = (0.78, 0.58)$ in Fig. 10, but they have notable BER difference in favor of the SIP scheme in Fig. 12. One possible explanation might be that the overall MSE is also important to determine the BER performance and the average MSE of the AGP scheme may not be well-controlled as the maximum MSE. To investigate this issue, we conduct simulations to show the average MSE performance in Fig. 14 using parameters given in Fig. 10. From Fig. 14, we observe that the proposed SIP scheme doesn't outperform the AGP scheme in terms of average MSE, because the SIP scheme targets the optimization of

the maximum sub-stream MSE shown in problem (16), not the average MSE. Hence, the comparison of the average MSE performance does not highly relate to that of the BER performance. We suppose that the reason is that although the average maximum MSE performance is similar, the maximum sub-stream MSE of the AGP scheme varies more widely than that of the SIP scheme, as can be observed from Fig. 10 where the variant range of the maximum sub-stream MSE is roughly bounded by the “curves of mean of Max MSE” for $(p_2, p_3) = (0, 0)$ and $(p_2, p_3) = (1, 1)$, and obviously the variant range of SIP is narrower than that of AGP. The variant range of the maximum sub-stream MSE indicates that the AGP scheme tends to generate larger maximum sub-stream MSE than the SIP scheme does in some poor cases, and the average BER performance is dominated by the large BERs resulted from poor-case maximum sub-stream MSEs, which will lead to a higher BER performance for the AGP scheme.

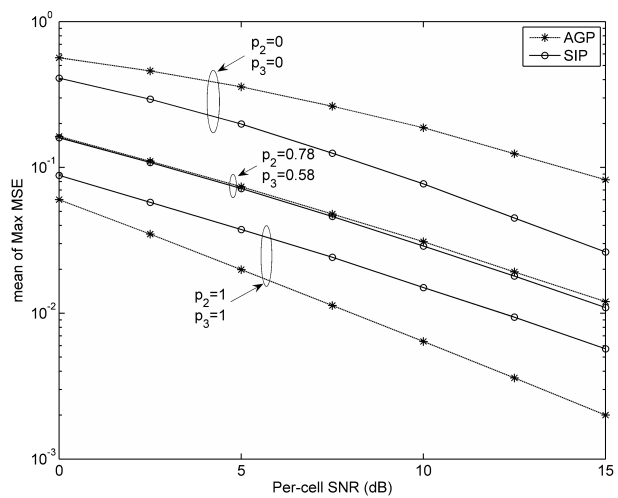


Fig. 10. Mean of the maximum of sub-stream MSEs for $B = 3$, $N_R = 2$ (perfect feedback).

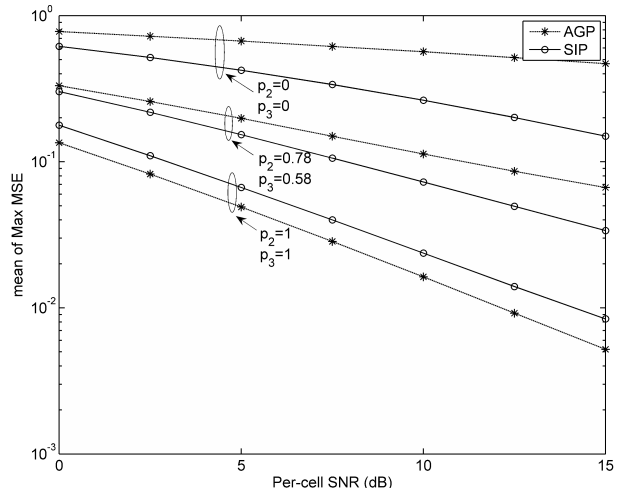


Fig. 11. Mean of the maximum of sub-stream MSEs for $B = 3$, $N_R = 4$ (perfect feedback).

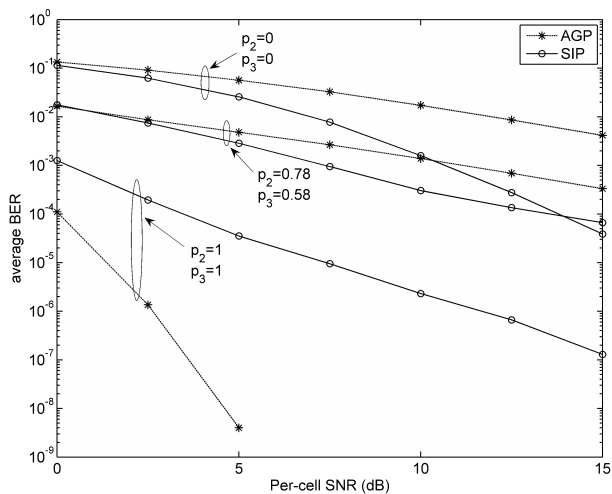


Fig. 12. Average BER for $B = 3$, $N_R = 2$ (perfect feedback).

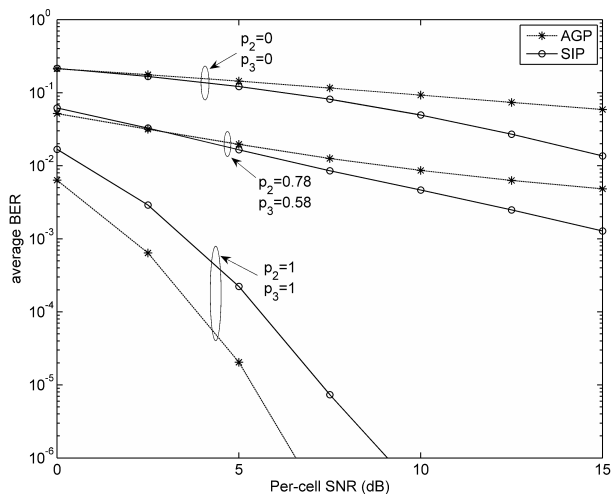


Fig. 13. Average BER for $B = 3$, $N_R = 4$ (perfect feedback).

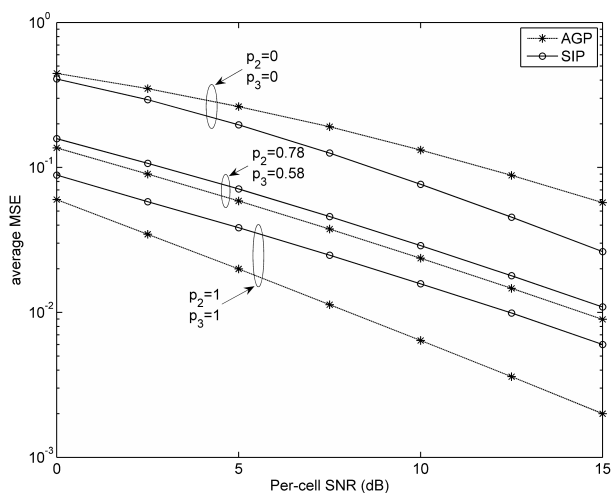


Fig. 14. Average MSE for $B = 3$, $N_R = 2$ (perfect feedback).

E. Performance of Finite Rate Feedback Systems

Since the proposed SIP scheme is developed under the assumption of perfect feedback, it is highly motivated to investigate whether the SIP scheme still works in case of practical

finite-rate feedback systems, i.e., the indices of the optimal codeword $\mathbf{W}_b^{\text{opt,cb}}$ rather than $\mathbf{W}_b^{\text{opt}}$ themselves are fed back. First, we investigate the choice of d in the codebook based feedback. In Fig. 15 and 16, average BER performance of the SIP and AGP schemes are shown for $B = 2$ ($p_2 = 0.78$) or $B = 3$ ($(p_2, p_3) = (0.78, 0.58)$), $N_R = 2$ and $d = 1 \sim 5$. We can observe in both figures that the performance gain suffers from a diminishing return as d increases and $d = 4$ seems to be a good tradeoff between performance improvement and feedback overhead. Moreover, $d = 4$ is a common assumption for codebook designs for BSs with 4 transmit antennas in the LTE-A system [3]. Thus in the following we provide new simulation results plotted in Fig. 17 to 24 for $d = 4$ to illustrate the performance degradation because of limited-bit feedback in compare with Fig. 6 to 13. In our simulations, precoder candidates in the codebook are randomly generated as matrix composed of orthogonal normalized vectors [35] for each channel realization. It can be observed from these figures that although the performance degradation is notable the gains of the SIP scheme shown in Fig. 6 to 13 are safely preserved.

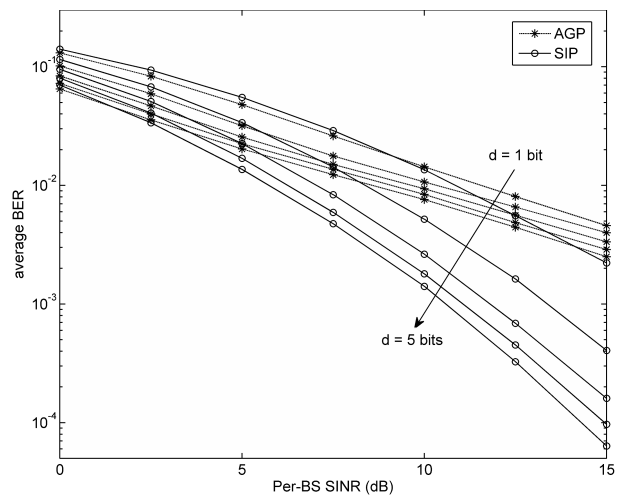


Fig. 15. Average BER for $B = 2$, $N_R = 2$, $d = 1 \sim 5$ (codebook based feedback).

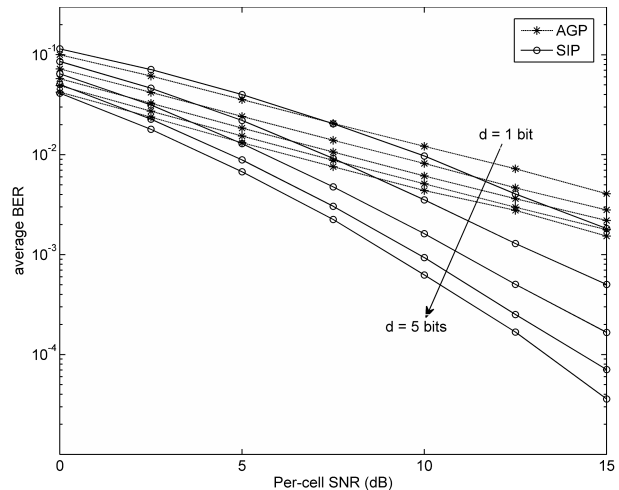


Fig. 16. Average BER for $B = 3$, $N_R = 2$, $d = 1 \sim 5$ (codebook based feedback).

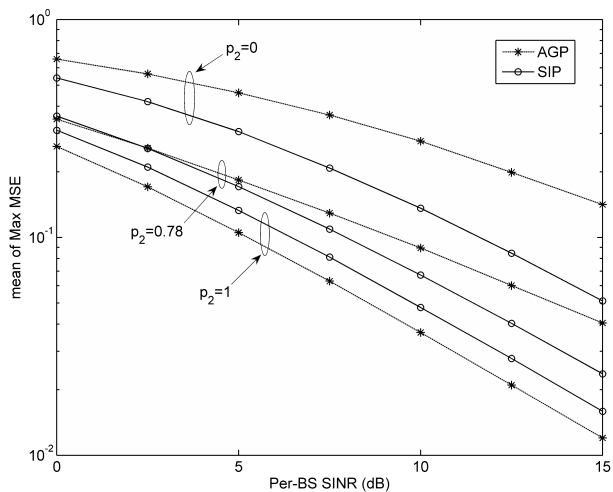


Fig. 17. Mean of the maximum of sub-stream MSEs for $B = 2$, $N_R = 2$, $d = 4$ (codebook based feedback).

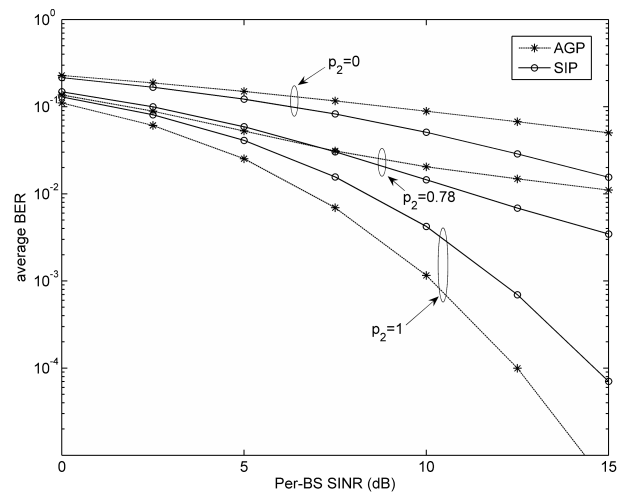


Fig. 20. Average BER for $B = 2$, $N_R = 4$, $d = 4$ (codebook based feedback).

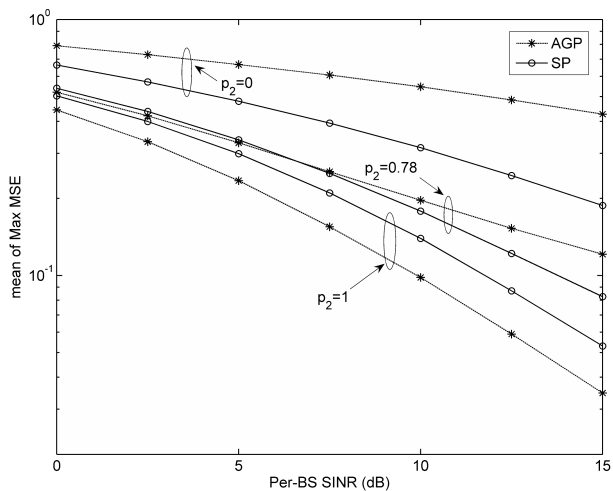


Fig. 18. Mean of the maximum of sub-stream MSEs for $B = 2$, $N_R = 4$, $d = 4$ (codebook based feedback).

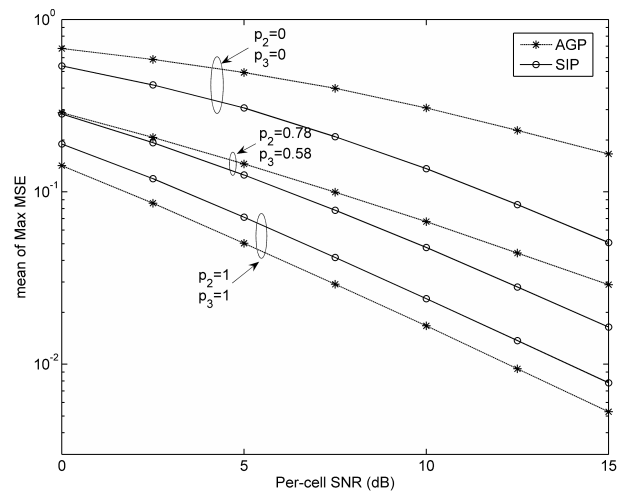


Fig. 21. Mean of the maximum of sub-stream MSEs for $B = 3$, $N_R = 2$, $d = 4$ (codebook based feedback).

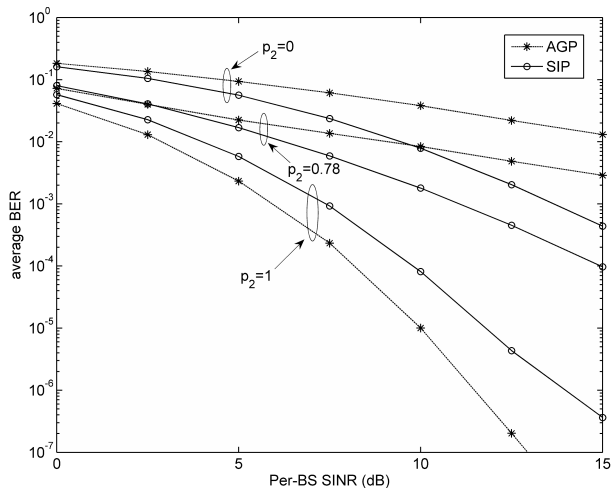


Fig. 19. Average BER for $B = 2$, $N_R = 2$, $d = 4$ (codebook based feedback).

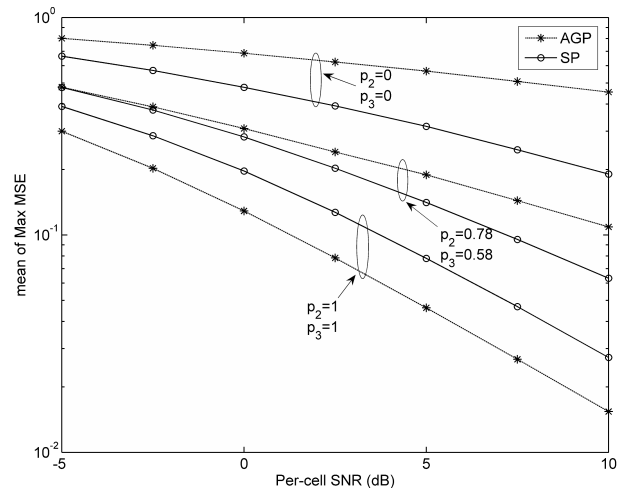


Fig. 22. Mean of the maximum of sub-stream MSEs for $B = 3$, $N_R = 4$, $d = 4$ (codebook based feedback).

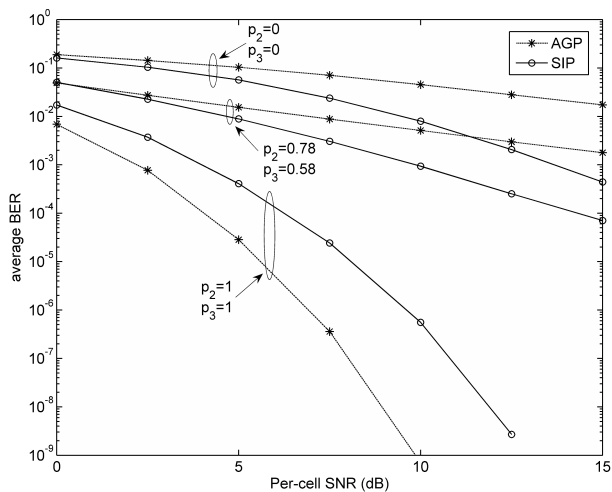


Fig. 23. Average BER for $B = 3$, $N_R = 2$, $d = 4$ (codebook based feedback).

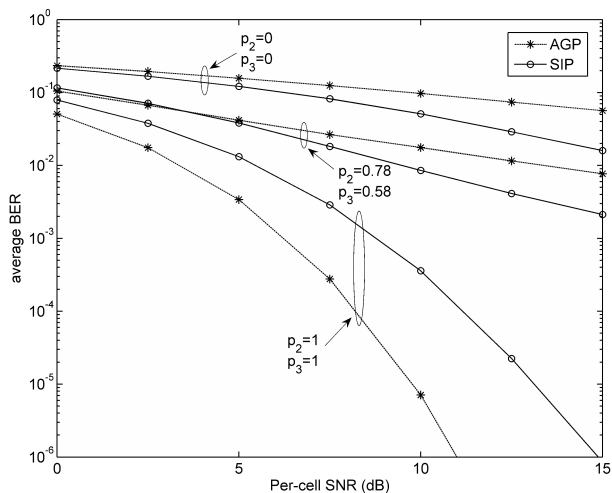


Fig. 24. Average BER for $B = 3$, $N_R = 4$, $d = 4$ (codebook based feedback).

F. Extension to the Multi-UE Scenario

Finally, we briefly discuss the further extension of the proposed SIP scheme to the multi-UE scenarios and more sophisticated evaluations using system-level simulations. When multiple UEs are involved, the Wiener filter in (18) can be replaced by a block diagonal matrix to reflect that individual UE's receive processing capability is captured by the corresponding block matrix and no receive cooperation is assumed among different UEs. Then the precoders for multiple UEs can be derived using the proposed SIP scheme. However, the closed-form expression for $\mathbf{W}_1^{\text{opt}}$ shown by (15) no longer exists. The algorithms for optimizing $\mathbf{W}_1^{\text{opt}}$ with various objective functions can be found in [23], which is beyond the scope of this paper and will be considered in the future works. Besides, the simulation results given in this paper are on a link-level basis. More sophisticated evaluations using system-level simulations [33] considering cell-edge/cell-average spectral efficiency, UE distribution, multi-cell scheduler, retransmission in case of packet error, traffic modeling, propagation channel modeling, channel estimation errors, BS power settings, etc.,

are beneficial to the investigation of the performance gain offered by the proposed scheme in more practical scenarios. Thus we will improve our simulation methods in the future works.

VI. CONCLUSION

In this paper, transmission precoder design based on a sequential and incremental approach for JT network MIMO systems with imperfect backhaul is studied. The conventional autonomous global precoding (AGP) scheme suffers from severe performance degradation in the event of partial JT and ST resulted from imperfect backhaul communications. A sequential and incremental precoding (SIP) scheme is proposed to overcome the drawbacks of the existing schemes. The key problem is first illustrated and solved with a two-BS JT system, and the results are then generalized to multi-BS JT network MIMO systems. Simulation results show that our scheme significantly outperforms the AGP scheme when practical backhaul link is considered. Finally, future works of extending the proposed SIP scheme to multi-UE scenarios and more sophisticated evaluations using system-level simulations are briefly discussed.

REFERENCES

- [1] D. Gesbert, S. Hanly, H. Huang, S. Shamai (Shitz), O. Simeone, and Y. Wei, "Multi-cell MIMO cooperative networks: a new look at interference," *IEEE J. Sel. Areas Commun.*, vol. 28, no. 9, pp. 1380–1408, Dec. 2010.
- [2] O. Somekh, O. Simeone, Y. Bar-Ness, A. M. Haimovich, and S. Shamai (Shitz), "Cooperative multicell zeroforcing beamforming in cellular downlink channels," *IEEE Trans. Inf. Theory*, vol. 55, no. 7, pp. 3206–3219, Jul. 2009.
- [3] 3GPP TR 36.814 V9.0.0, "Further advancements for E-UTRA physical layer aspects," *Tech. Rep.*, Mar. 2010.
- [4] J. Zhang, R. Chen, J. G. Andrews, A. Ghosh, and R. W. Heath, "Networked MIMO with clustered linear precoding," *IEEE Trans. Wireless Commun.*, vol. 8, no. 4, pp. 1910–1921, Apr. 2009.
- [5] H. Dahrouj and W. Yu, "Coordinated beamforming for the multicell multi-antenna wireless system," *IEEE Trans. Wireless Commun.*, vol. 9, no. 5, pp. 1748–1759, May 2010.
- [6] L. Venturino, N. Prasad, and X. Wang, "Coordinated linear beamforming in downlink multi-cell wireless networks," *IEEE Trans. Wireless Commun.*, vol. 9, no. 4, pp. 1451–1461, Apr. 2010.
- [7] C. B. Chae, S. Kim, and R.W. Heath, "Network coordinated beamforming for cell-boundary users: linear and nonlinear approaches," *IEEE Selected Topics in Signal Process.*, pp. 1094–1105, Dec. 2009.
- [8] S. Shamai (Shitz) and B. Zaidel, "Enhancing the cellular downlink capacity via co-processing at the transmitting end," *IEEE Vehicular Technology Conference (VTC)*, vol.3, pp. 1745–1749, May 2001.
- [9] N. Jindal, S. Vishwanath, and A. Goldsmith, "On the duality of Gaussian multiple-access and broadcast channels," *IEEE Trans. Inf. Theory*, vol. 50, no. 5, pp. 768–783, May 2004.
- [10] W. Yu and T. Lan, "Transmitter optimization for the multi-antenna downlink with per-antenna power constraints," *IEEE Trans. Sig. Process.*, vol. 55, no. 6, pp. 2646–2660, Jun. 2007.
- [11] M. H. M. Costa, "Writing on dirty paper," *IEEE Trans. Inf. Theory*, vol. 29, no. 3, pp. 439–441, May 1983.
- [12] H. Huh, H. Papadopoulos, and G. Caire, "MIMO broadcast channel optimization under general linear constraints," *IEEE Int. Symp. Inf. Theory (ISIT)*, pp. 2664–2668, June 2009.
- [13] D. P. Palomar and Y. Jiang, "MIMO transceiver design via majorization theory," *Found. Trends Commun. Inf. Theory*, vol. 3, no. 4, pp. 331–551, Nov. 2006.
- [14] P. Marsch and G. Fettweis, "On downlink network MIMO under a constrained backhaul and imperfect channel knowledge," *IEEE Global Telecommun. Conf. (Globecom)*, pp. 5059–5064, Nov. 2009.
- [15] Orange, Telefónica, "R1-111174: Backhaul modelling for CoMP," 3GPP TSG-RAN1#64 meeting, Taipei, Taiwan, Feb. 2011.

- [16] R. Zakhour, D. Gesbert, "Optimized Data Sharing in Multicell MIMO With Finite Backhaul Capacity," *IEEE Trans. Sig. Process.*, vol. 59, no. 12, pp. 6102-6111, Dec. 2011.
- [17] MCC Support, "R1-110611: Final Report of 3GPP TSG RAN WG1 #63bis v1.0.0," 3GPP TSG-RAN1#64 meeting, Taipei, Taiwan, Feb. 2011.
- [18] MCC Support, "R1-111226: Final Report of 3GPP TSG RAN WG1 #64 v1.0.0," 3GPP TSG-RAN1#65 meeting, Barcelona, Spain, May 2011.
- [19] Orange, Deutsche Telekom, NTT DOCOMO, Telecom Italia, Telefónica, Vodafone, "R1-110546: Views on CoMP evaluation methodology," 3GPP TSG-RAN1#63bis meeting, Dublin, Ireland, Jan. 2011.
- [20] Samsung, "RP-101425: Revised SID Proposal: Coordinated Multi-Point Operation for LTE," 3GPP TSG RAN#50 meeting, Istanbul, Turkey, Dec. 2010.
- [21] Ericsson, ST-Ericsson, "R1-110452: Deployment and backhaul constraints for CoMP," 3GPP TSG-RAN1#63bis meeting, Dublin, Ireland, Jan. 2011.
- [22] 802.20 Permanent Document, "802.20 Evaluation Criteria (V1.0)", Sept. 2005.
- [23] D. P. Palomar, M. A. Lagunas, and J. M. Cioffi, "On the optimal structure of transmit-receive linear processing for MIMO systems," IEEE 40th Annu. Allerton Conf. Commun., Contr., Comput., Oct. 2002.
- [24] S. Zhou, J. Gong, Z. Niu, Y. Jia, P. Yang, "A Decentralized Framework for Dynamic Downlink Base Station Cooperation," IEEE Global Telecommunications Conference (GLOBECOM), pp. 1-6, Dec. 2009.
- [25] J. Moon; D. Cho, "Efficient Cell-Clustering Algorithm for Inter-Cluster Interference Mitigation in Network MIMO Systems," *IEEE Communications Letters*, vol. 15, no. 3, pp. 326-328, Mar. 2011.
- [26] Samsung, "R1-114223: Discussion on the Size of CoMP Measurement Set," 3GPP TSG RAN1#67 meeting, San Francisco, USA, Nov. 2011.
- [27] P. Skillermarck, M. Almgren, D. Astely, M. Lundevall, M. Olsson, "Simplified Interference Modeling in Multi-Cell Multi-Antenna Radio Network Simulations," IEEE Vehicular Technology Conference (VTC), pp. 1886-1890, May 2008.
- [28] 3GPP TS 23.401 (V8.1.0), "General Packet Radio Service (GPRS) enhancements for Evolved Universal Terrestrial Radio Access Network (E-UTRAN) access (Release 8)", pp. 129, Mar. 2008.
- [29] I. S. Gradshteyn, I. M. Ryzhik, *Tables of Integrals, Series, and Products (7th ed.)*. Academic Press. 2007.
- [30] D. P. Palomar, J. M. Cioffi, and M. A. Lagunas, "Joint Tx-Rx beamforming design for multicarrier MIMO channels: a unified framework for convex optimization," *IEEE Trans. Sig. Process.*, vol. 51, no. 9, pp. 2381-2401, Sept. 2003.
- [31] D. Tse and P. Viswanath, *Fundamentals of Wireless Communication*. Cambridge University Press, 2005.
- [32] P. Viswanath and V. Anantharam, "Optimal sequences and sum capacity of synchronous CDMA systems," *IEEE Trans. Inf. Theory*, vol. 45, pp. 1984-1991, Sept. 1999.
- [33] 3GPP TR 36.819 (V11.0.0), "Coordinated multi-point operation for LTE physical layer aspects (Release 11)", Sept. 2011.
- [34] S. Boyd and L. Vandenberghe, *Convex Optimization*. Cambridge University Press, 2004.
- [35] W. Santipach and M. Honig. "Asymptotic capacity of beamforming with limited feedback." IEEE Int. Symp. Inf. Theory (ISIT). pp. 289, June 2004.